ALKALINE TREATMENT OF SUGARCANE BAGASSE FIBERS FOR BIOCOMPOSITE APPLICATIONS

ABDELHAY AIT-ABDELLAH,[*] OUMAIMA BELCADI,[*,**] MOHAMED AIT BALLA,[*,***] HAMID BOUNOUADER,[****] HAMID KADDAMI,[*****] NOURREDINE ABIDI[******] and FATIMA-EZZAHRA ARRAKHIZ[*]

[*]*Laboratory Materials, Signals, Systems and Physical Modeling, Faculty of Science, Ibn Zohr University, Dakhla, B.P. 8106, Agadir 80000, Morocco*
[**]*Laboratory of Mechanics of Normandy (LMN), INSA Rouen Normandy, University of Normandy, Rouen 76000, France*
[***]*Laboratory of Engineering of Polymer Materials, INSA Lyon, University of Lyon, CNRS, UMR 5223, Villeurbanne 69621, France*
[****]*EUROMED Research Center, School of Engineering Biomedtech, University of Fes, Morocco*
[*****]*Laboratory of Innovative Materials for Energy and Sustainable Development (IMAD-Lab), Faculty of Sciences and Technologies, Cadi Ayad University, Marrakech 40000, Morocco*
[******]*Fiber and Biopolymer Research Institute, Department of Plant and Soil Science, Texas Tech University, 1001 East Loop 289, Lubbock, TX 79403, USA*
✉ *Corresponding author: F.-E. Arrakhiz, f.arrakhiz@uiz.ac.ma*

Received September 8, 2023

This study investigates the mechanical, structural, morphological, and thermal properties of chemically treated and untreated sugarcane bagasse fibers (SCB). Various concentrations of NaOH were used for the treatment over four hours. The main goal was to investigate the impact of alkali treatment on the overall properties of SCB fibers intended for composite applications. The results indicated that the crystallinity index, thermal stability, and mechanical properties were improved with the treatment, and this is due to the removal of impurities initially present on the outer surface of the SCB fiber and the reduction of amorphous components. This improvement may facilitate better adhesion between the SCB fibers and the polymeric matrices in biocomposite applications. However, it is important to determine the optimal concentration of NaOH that improves the properties of the SCB fiber without damaging the fiber's structure.

Keywords: sugarcane bagasse fiber, alkali treatment, chemical composition, mechanical properties, thermal stability, biocomposites

INTRODUCTION

Growing concerns over the depletion of fossil fuels and climate change have sparked interest in substituting synthetic fibers in polymeric composites with natural plant fibers. Natural fibers offer several advantages over synthetic fibers, such as low density, recyclability, biodegradability, availability, moderate strength and modulus, cost-effectiveness, user-friendliness, and less energy consumption.[1] Due to these characteristics, various applications of natural fiber-based composites have been explored, such as in construction industry, military applications, automobile, aircraft and railway wagon construction, consumer products, and packaging.[2] However, natural fibers also possess hydrophilic characteristics, due to the presence of hydroxy groups (-OH), which may limit their utility in certain applications. Additionally, when considering composites, the hydrophobic matrix and the hydrophilic fiber have poor interfacial adhesion.[3] These drawbacks can be overcome by chemical treatments of the fibers, such as

alkalization, benzoylation, acetylation, and silane treatment.[4]

Alkali treatment, or alkalization, is the most efficient and cost-effective method to increase the compatibility between fibers and the matrix. It involves removing lignin, hemicelluloses, waxes, and fats from the outer surface of lignocellulosic fibers using an alkali solution.[5] Previous studies have investigated the effect of alkali treatment on the physico-chemical and mechanical properties of various natural fibers, including bamboo,[6,10] jute,[7] kenaf,[5] alfa fiber,[8] Cabuya[9] *etc*.

This research aims to examine how treating sugarcane bagasse fibers (SCB) with varying concentrations of NaOH (6%, 12%, and 18%) affects their structural, morphological, thermal, and tensile properties. The ultimate objective is to determine the optimal NaOH concentration that enhances the fiber properties without compromising their integrity. By achieving this goal, the interfacial adhesion between the SCB fibers and polymeric matrices will be improved, ensuring good adhesion in composite applications.

EXPERIMENTAL

Fiber extraction

The sugarcane bagasse (SCB) waste was collected from a local area in Agadir, Morocco. The extracted fibers were thoroughly cleansed with water to eliminate any external impurities, and then sun-dried for 48 h. Next, the fibers were ground with a mechanical grinder for a few minutes and sifted to obtain uniform fractions that were 1.5 mm long and 200 µm wide.

Alkali treatment of fiber

The SCB fibers were ground and subsequently soaked in NaOH solution at varying concentrations (6%, 12%, and 18%) for approximately 4 hours at room temperature (25 °C), at a solution to fiber ratio of 20:1. After the treatment, the fibers were carefully rinsed numerous times with distilled water and dried at 25 °C for 48 hours. Figure 1 shows the difference in appearance between untreated and alkali-treated fibers.

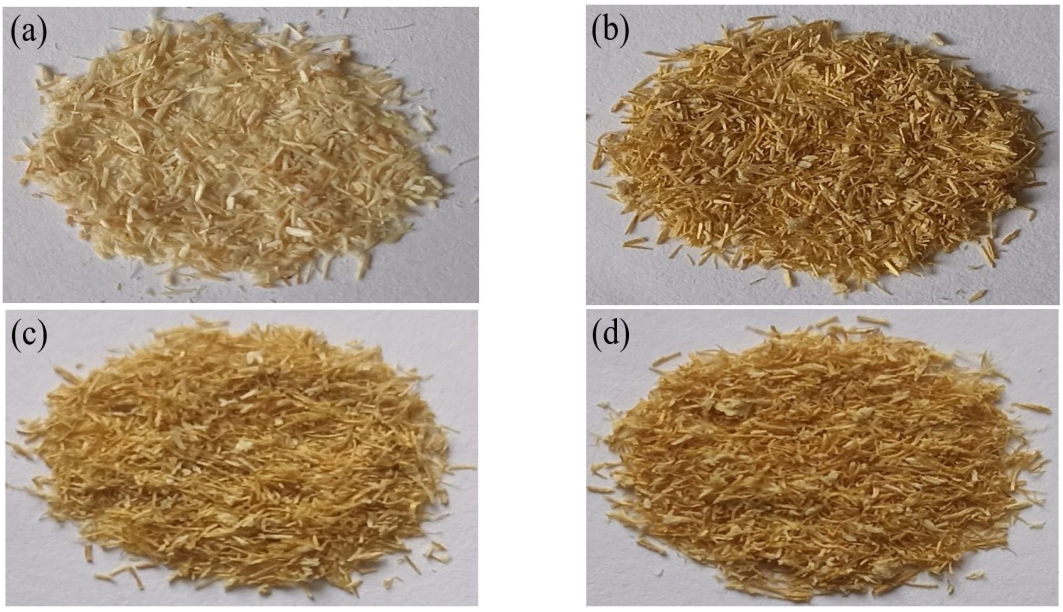

Figure 1: Sugarcane bagasse fiber (a) untreated, (b) 6% NaOH treated, (c) 12% NaOH treated, and (d) 18% NaOH treated

Characterization

Chemical composition of SCB fibers

The analysis of the chemical composition was done following the French standard T 12011. The Klason method was used to determine the amount of lignin in fibers. To do this, 1 g of ground fibers were suspended in 72% sulfuric acid for 2 hours and subjected to hydrolysis, reflux, filtration, and washing. This process helps in determining the amount of lignin present by measuring the weight of the residue left after washing.

Before the holocellulose extraction, the fibers underwent a 6, 12, and 18% NaOH treatment, then were filtered through a 100 µm mesh and washed several times. The resulting brown pulp was then bleached with sodium chlorite in a buffered environment at 70 °C, filtered, and washed to yield holocellulose. The purification of cellulose was done by dissolving the hemicelluloses in an alkaline solution, neutralizing it with acetic acid (50% v/v), and then centrifuging it for 30 minutes at 5000 rpm. After

that, the solution was subjected to ethanol treatment, filtration, and washing with absolute ethanol.

Fourier transform infrared spectroscopy

Fourier transform infrared spectroscopy (FTIR) measurements were conducted using a Perkin-Elmer 1000 Spectrometer. The spectral range covered a wide range from 450 to 4000 cm^{-1}, allowing for a detailed analysis of the sample's properties. The spectrometer was set at a high resolution of 4 cm^{-1}, ensuring accurate and precise measurement results. An accumulation of 32 scans was performed to increase the signal-to-noise ratio and minimize the effect of random noise in the measurements.

NMR (CP-MAS) spectroscopy

To obtain a detailed analysis of the chemical composition of untreated and alkali-treated SCB fibers, 13C CP-MAS NMR spectra were collected using a JOEL 600, 300 MHz solid-state NMR spectrometer. The operating frequency for 13C nuclei was fixed at 75.46 MHz, allowing for accurate and precise measurements. The samples were spun with a filled 5 mm rotor at a spinning rate of 5 kHz at room temperature, ensuring uniformity in the sample and minimizing any variations that could affect the results.

Scanning electron microscopy analysis (SEM)

To observe and understand the surface morphology of SCB fibers, we employed a JOEL scanning electron microscope operating at a voltage of 7 kV. This provided valuable insights into their physical structure and properties. Furthermore, we performed elemental analysis of the fiber surface using energy-dispersive X-ray spectroscopy (SEM-EDX), which enabled us to identify and quantify the elements present on the surface of the fibers.

X-ray diffraction (XRD) analysis

X-ray diffraction (XRD) analysis was conducted to determine crystallographic properties of untreated and alkali-treated SCB fibers, such as percentage crystallinity (%Cr), crystallinity index (CrI), and crystalline size (CS). The XRD measurements were carried out using a Rigaku Smartlab series BD67000407-01 X-ray diffractometer with Cu Kα radiation (1.5406 A˚), at operating conditions of 40 kV and 50 mA. The diffractograms were collected with a step scanning mode of 2θ (diffraction angle) ranging from 5° to 60°, with a scanning rate of 0.02° at room temperature. %Cr was calculated using Equation (1):[11]

$$\%C_r = \frac{I_{002}}{I_{002}+I_{am}} \times 100 \quad (1)$$

where I_{200} is the intensity of the crystalline phase peak at around 22˚ and I_{am} is the intensity of the amorphous phase peak at around 18˚.

The crystallinity index (C_rI) of untreated and treated SCB fibers was computed through Segal's expression (2):[12]

$$C_rI = \frac{I_{002}-I_{am}}{I_{002}} \times 100 \quad (2)$$

The crystallite size (CS) was determined using Scherrer's Equation (3):[13]

$$CS = \frac{K\times\lambda}{\beta\times\cos\theta} \times 100 \quad (3)$$

where K = 0.94 is the Scherrer's constant, β is the peak's full width at half-maximum and λ represents the wavelength of the radiation.

Thermogravimetric analysis (TGA)

Thermogravimetric analysis (TGA) was utilized to assess the thermal stability of the treated and untreated SCB fibers. It was performed using a TGA 55 Discovery instrument, with a heating rate of 10 °C/min within a temperature range of 30 °C to 700 °C under a nitrogen atmosphere. To calculate the kinetic activation energy (E_α) of the untreated and alkali-treated fibers, Broido's equation (Eq. (4)) was employed:[14]

$$\ln\left(\ln\frac{1}{y}\right) = -\frac{E_a}{R}\left(\frac{1}{T}+k\right) \quad (4)$$

where R represents the universal gas constant (8.32 J/mol.K), T is the temperature in Kelvin, K is a constant, γ represents normalized weight (w_t/w_i), w_t is the weight of the sample at any time t, and w_i is the initial weight of the sample.

Physical analysis

Density measurement

The density of both untreated and alkali-treated SCB fibers was determined using the pycnometer method following ASTM D578-89 standard. Xylene was used as an immersion liquid, and the density (ρf) was calculated using Equation (5).

$$\rho_f = \frac{W_2-W_1}{(W_3-W_1)-(W_4-W_2)} \times \rho_X \quad (5)$$

where W_1 is the mass of the empty pycnometer, W_2 is the mass of the pycnometer filled with chopped fiber, W_3 is the mass of the pycnometer filled with xylene at 25 °C, W_4 is the mass of the pycnometer filled with chopped fibers, and xylene at 25 °C. ρ_X is the density of xylene (0.866 $g.cm^{-3}$ at 25 °C), and ρ_f is the density of SCB fibers in $g.cm^{-3}$.

Diameter measurement

The average diameter of untreated and treated SCB fibers was determined using an Optical microscope. Five measurements were taken along each of the twenty randomly selected fibers from each sample to obtain the average diameter.

Mechanical properties

Tensile tests were conducted on untreated and alkali-treated SCB fibers to measure the mechanical properties, using a universal testing machine with a 5KN capacity load cell, following the ASTM D3822-

07 standard. The gauge length was set to 30 mm and the testing was performed at a crosshead speed of 1.5 mm/min. The fibers were maintained and clued in a frame of paper and mounted between clamps of the tensile tester, as illustrated in Figure 2.

Multiscale modeling: finite element analysis

This section proposes a multiscale modeling approach using the Digimat-FE tool to evaluate the performance of untreated and alkali-treated SCB fibers incorporated in a polypropylene (PP) thermoplastic matrix. The aim is to assess their suitability for various composite applications.

Digimat-FE is a software tool used for analyzing and simulating the behavior of composites (heterogenous environments) by the use of finite element analysis (FEA). This software enables the generation of a realistic three-dimensional structure known as a representative volume element (RVE). Once the RVE is created and meshed, appropriate boundary conditions are applied, and a load is imposed on the structure. Digimat-FE offers various types of boundary conditions, including Dirichlet, periodic, or mixed conditions. For this particular investigation, periodic boundary conditions were employed. The FEA was performed using a uniaxial tensile loading aligned with the fiber orientation direction, as it is reported that for high-volume fractions (<20 wt%), the fibers tend to align with the fabrication flow direction.[15]

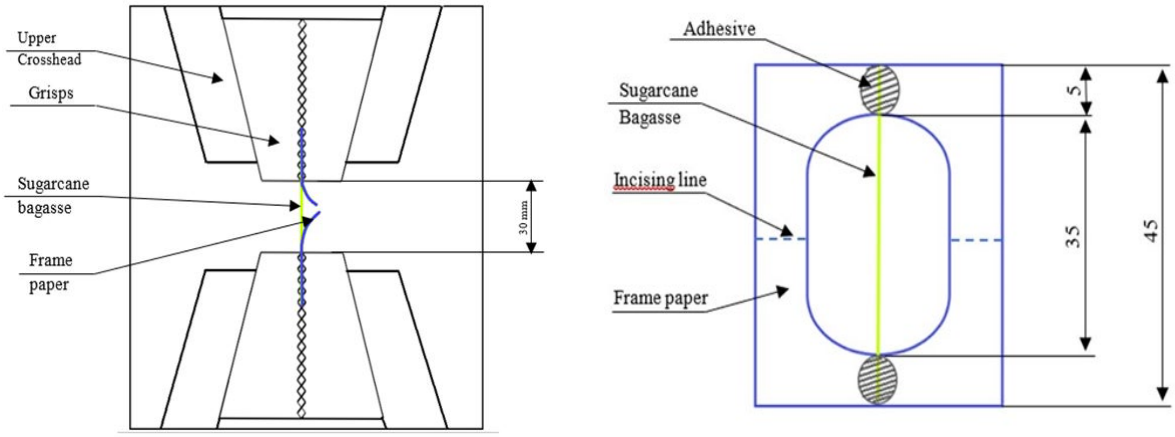

Figure 2: Tensile test setup of SCB fibers

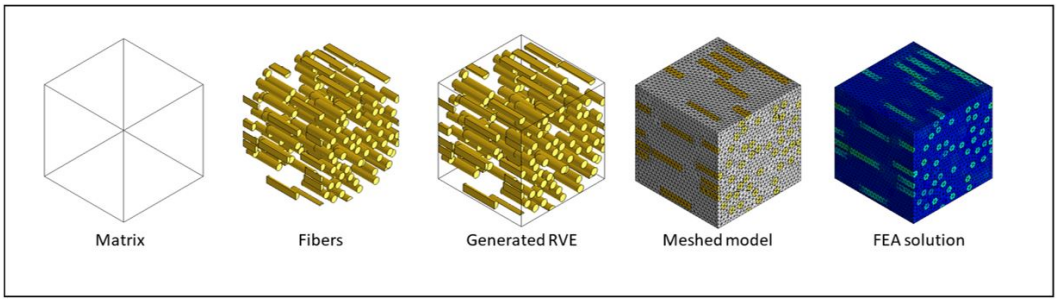

Figure 3: Finite element analysis process by Digimat-FE

Table 1
Input parameters of finite element analysis (material's inputs)

Phase	PP	SCB fibers
Density (g/cm^3)	0.9	Table 8
Poisson's ratio	0.4 [16]	0.3
Young's modulus (GPa)	1.3 [16]	Table 9
Phase type	Matrix	Inclusion
Volume fraction	0.85	0.15
Fiber shape	-	Cylindrical
Fiber diameter (mm)	-	Table 8
Fiber size (mm)	-	1.5 [17]
Fiber orientation	-	90°

The last step consists of simulating the overall behavior of the composite by averaging the stress and strain fields obtained at the microscopic scale under the applied boundary conditions. The FEA process is presented in Figure 3 and materials and microstructure input parameters are summarized in Table 1.

RESULTS AND DISCUSSION

Chemical composition

The results of the chemical composition of untreated and alkali-treated SCB fibers using different concentrations of NaOH are shown in Table 2. The results show that the untreated SCB fibers possess a high cellulose content of 36.62%, whereas hemicelluloses and lignin contents were 28.42% and 15.51%, respectively. The high cellulose content indicates that SCB fibers might be a promising source of cellulose. Upon treatment with NaOH, the cellulose content increased significantly, which can be attributed to the removal of lignin, hemicelluloses, and other non-cellulosic compounds that are soluble in NaOH.

The results demonstrate that lignin content was reduced by 8.43%, 6.21%, and 7.59% for NaOH concentrations of 6%, 12%, and 18%, respectively. On the other hand, hemicelluloses were found to be more sensitive to the action of alkali treatment, with reductions of 12.27%, 8.14%, and 9.52% for NaOH concentrations of 6%, 12%, and 18%, respectively. Thus, an increase in NaOH concentration resulted in decreased lignin and hemicelluloses contents. Furthermore, the extractives and ash content also showed a continuous decrease with an increase in alkali concentration.

The moisture content of the SCB fibers decreased from 11.23% for untreated fibers to 10.13%, 9.42%, and 10.08% for NaOH concentrations of 6%, 12%, and 18%, respectively. This reduction can be attributed to the removal of amorphous lignin and hemicelluloses. Table 3 provides a comparison of the chemical composition of raw SCB fibers with other important natural fibers.

Fourier transform infrared spectroscopy (FT-IR)

Changes in chemical composition following alkali treatment were investigated by FTIR as well. Figure 4 shows the spectra of untreated and treated SCB fibers with 6, 12, and 18% NaOH respectively. The IR vibrations present in the spectra and their assignments are summarized in Table 4.

The absorption band around 3410 cm^{-1} is attributed to the hydrogen-bonded O-H stretching of cellulose, which is present in all natural fibers.[25] The vibration observed at 2924 cm^{-1} is assigned to the C-H stretching vibration of the –CH_2– group of cellulose and hemicelluloses,[26] while the vibration at 2854 cm^{-1} could be assigned to hemicelluloses.[27]

The vibration 1737 cm^{-1} observed in untreated fiber is assigned to the stretching of carbonyl groups (C=O) in ester linkages of carboxylic groups of lignin.[28] However, Loganathan *et al*. have assigned this vibration to C=O stretching of hemicelluloses.[29] This vibration is absent in alkali-treated fibers due to the partial removal of lignin and hemicelluloses components. The bending vibration of absorbed water is observed at 1640 cm^{-1} in the spectra of all-fiber samples.[30]

The vibration 1515 cm^{-1} in the spectra of untreated fiber, attributed to the aromatic ring C=C stretching vibrations of lignin, considerably decreases in alkali-treated fibers due to the partial removal of the lignin component.[31] The intensity of vibration observed at 1251 cm^{-1}, which corresponds to C-O stretching vibration of acetyl groups in lignin and hemicelluloses, was sharply decreased after alkali treatment due to the partial removal of the lignin and hemicelluloses components.[32]

Table 2
Chemical composition of untreated and alkali-treated SCB fibers

Sample	Cellulose (%)	Hemicelluloses (%)	Lignin (%)	Extractible (%)	Ash (%)	Moisture (%)
Untreated	36.62	28.42	15.51	6.87	1.10	11.23
6% NaOH	61.62	12.27	8.43	5.53	1.03	10.13
12% NaOH	69.57	8.14	6.21	4.24	0.94	09.42
18% NaOH	67.24	9.52	7.59	3.91	0.88	10.08

Table 3
Chemical composition of raw SCB and other natural fibers

Fiber	Cellulose (%)	Hemicelluloses (%)	Lignin (%)	Wax (%)	Ash (%)	Moisture (%)
Kenaf [18]	45–57	8–13	21.5	0.8	2–5	6.2–12
Jute [19]	61–71.5	17.9–22.4	11.8–13	0.5	0.5–2	12.5–13.7
Hemp [19,20]	70.2–74.4	17.9–22.4	3.7–5.7	0.8	0.8	6.2–12
Bamboo [21]	26–43	30	1–31	–	–	9.16
Sisal [22,23]	78	10	8	2	1	11
Cotton [19]	82.7–90	3	–	0.6	–	7.85–8.5
Coconut tree leaf sheath[24]	27.7	14	27.7	–	–	4.7
Sugarcane bagasse	36.62	30.42	16.51	1.1	7.87	4.94

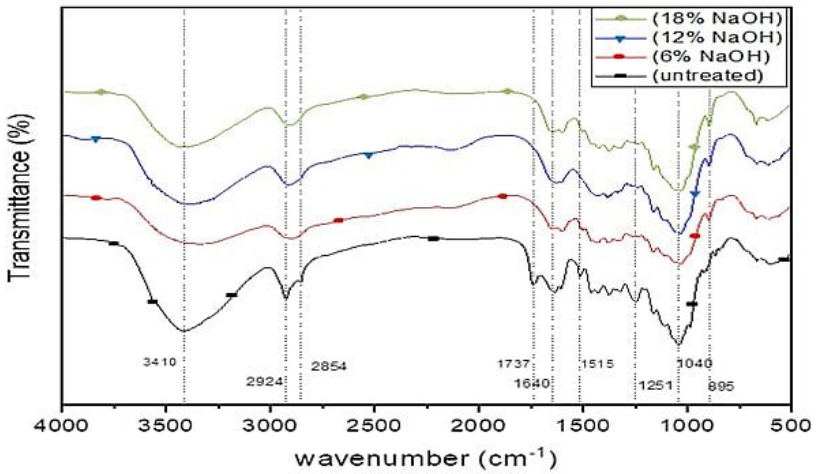

Figure 4: FTIR spectra of untreated and NaOH-treated sugarcane bagasse fibers

Table 4
Peak positions and assignments of chemical groups in untreated and treated SCB fibers

Peak position (wavenumber cm^{-1})	Assignments
3410	OH-stretching of cellulose [25]
2924	CH stretching of cellulose [26]
2854	CH stretching of hemicelluloses [27]
1737	Carbonyl groups (C=O) stretching of hemicelluloses and lignin [28]
1640	Bending vibration of absorbed water [30]
1515	Aromatic ring C=C stretching vibration for lignin [31]
1251	C-O stretching vibration of acetyl groups in lignin and hemicelluloses [32]
1040	C-O-C pyranose ring skeletal vibration of cellulose [33]
895	β-glucosidic linkages between glucose units [30]

The vibration observed around 1040 cm^{-1} indicates the absorption of C-O-C pyranose ring skeletal vibration of cellulose,[33] while the vibration observed at 895 cm^{-1} corresponds to β-glucosidic linkages between the glucose units.[30] The FTIR analysis confirms the results obtained from the chemical analysis and shows the presence of cellulose, hemicelluloses, and lignin. Similar observations have been reported for jute fiber[7] and for Eucalyptus fiber.[34]

NMR (CP-MAS) spectroscopy

The 13C CPMAS NMR analysis is another technique used to investigate the changes in the chemical composition of untreated and alkali-treated SCB fiber. The results shown in Figure 5 confirm the presence of acetyl groups in

hemicelluloses at 20.34 ppm and methoxyl groups (OCH3) in lignin in the untreated fiber spectrum at 55.80 ppm.[35] The peaks in the carbohydrate moiety are also observed in both spectra, between 60 and 110 ppm. The peaks at 64 ppm and 62 ppm are attributed to the C6 carbon of crystalline and amorphous cellulose, respectively.[36]

The peaks in the 71–75 ppm region are attributed to C2, C3, and C5 carbons of cellulose, and the peak at 105.23 ppm is assigned to cellulose C1. The separation peaks for amorphous and crystalline carbons could be detected. The peaks at 89 ppm and 84 ppm are assigned to C4 of highly ordered and disordered cellulose of the crystallite, respectively.

The disappearance of peaks at 55.80 and 20.34 ppm in the treated fiber spectrum indicates that both hemicelluloses and lignin were partially removed by the alkali treatment, while cellulose was affected as well. These results obtained with 13C CPMAS NMR analysis are consistent with those obtained from FTIR analysis, and similar results were reported for alfa fiber.[37]

Morphology analysis

Scanning electron microscopy analysis (SEM)

The images in Figure 6 show the differences between untreated and alkali-treated SCB fibers in terms of surface morphology. The SEM of untreated SCB fibers shows that the surface is covered with substances that could be lignin, hemicelluloses, and non-cellulosic compounds. These substances can hinder the bonding between the fiber and the matrix. However, treatment with NaOH solutions led to the removal of these impurities, resulting in smoother and cleaner fiber surfaces.

In particular, the SEM image of treated SCB fiber with 6% NaOH shows a slightly smoother surface, indicating a partial removal of non-cellulosic compounds.

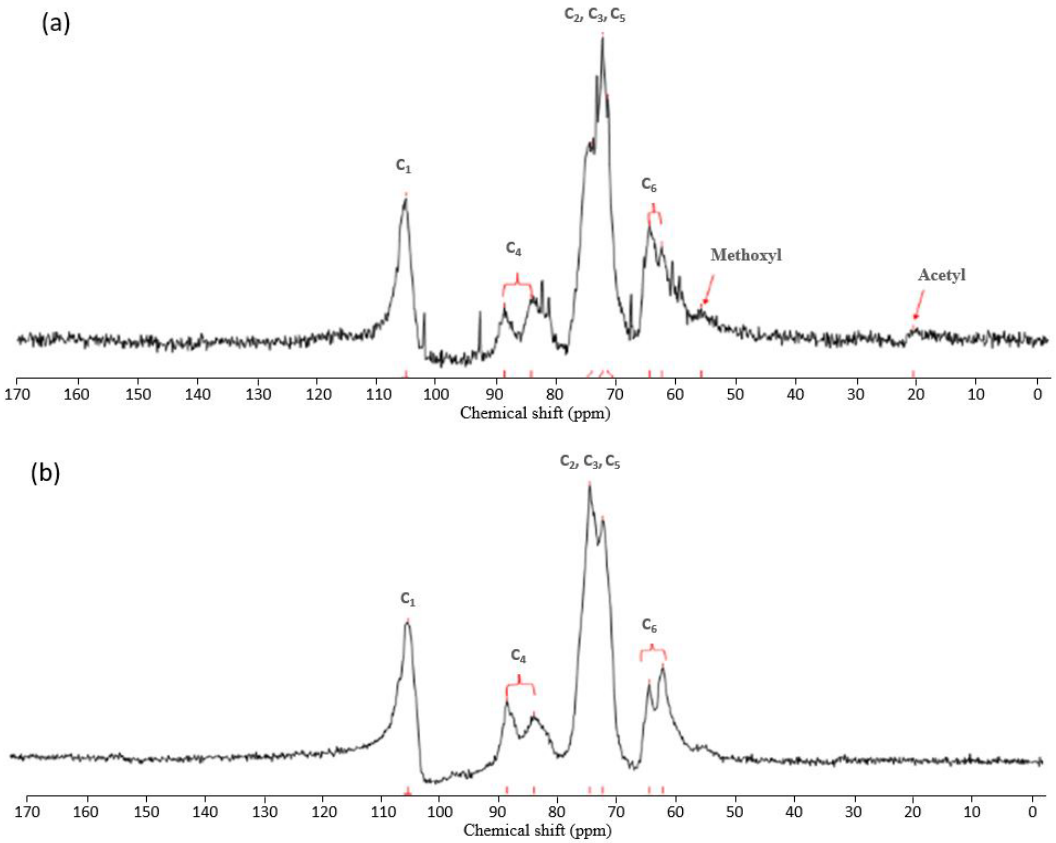

Figure 5: 13C CP-NMR spectra of sugarcane bagasse fibers (a) untreated, and (b) 18% alkali-treated fibers

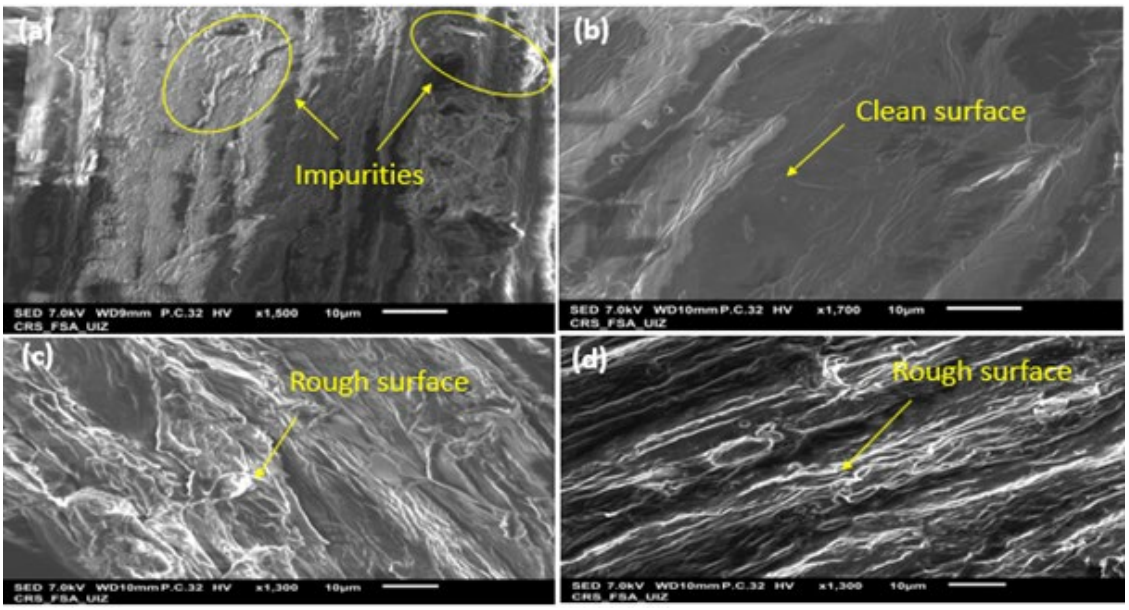

Figure 6: SEM micrographs of (a) untreated, (b) 6%, (c) 12% and (d) 18% NaOH treated SCB fibers

The surface of treated fibers with 12% NaOH solution appears even smoother and free from non-cellulosic impurities. The treatment with a high concentration of NaOH led to the appearance of microfibrils on the surface of the fibers. This rough surface is generally preferred to improve interfacial bonding between fibers and the polymer matrix.[38] Similar behavior was observed for *Pinus* fibers.[25] Overall, the SEM images confirm the effectiveness of the alkali treatment in removing impurities and improving the surface morphology of the SCB fibers.

Energy dispersive X-ray analysis (EDX)

The results of the EDX analysis of untreated and alkali-treated SCB fibers are summarized in Figure 7. The surface of the fibers contains high concentrations of carbon and oxygen, along with small traces of other elements, such as Na, Mg, Si, Cl, and K. However, after treatment with NaOH, the levels of Na, Mg, Si, Cl, and K are significantly reduced.

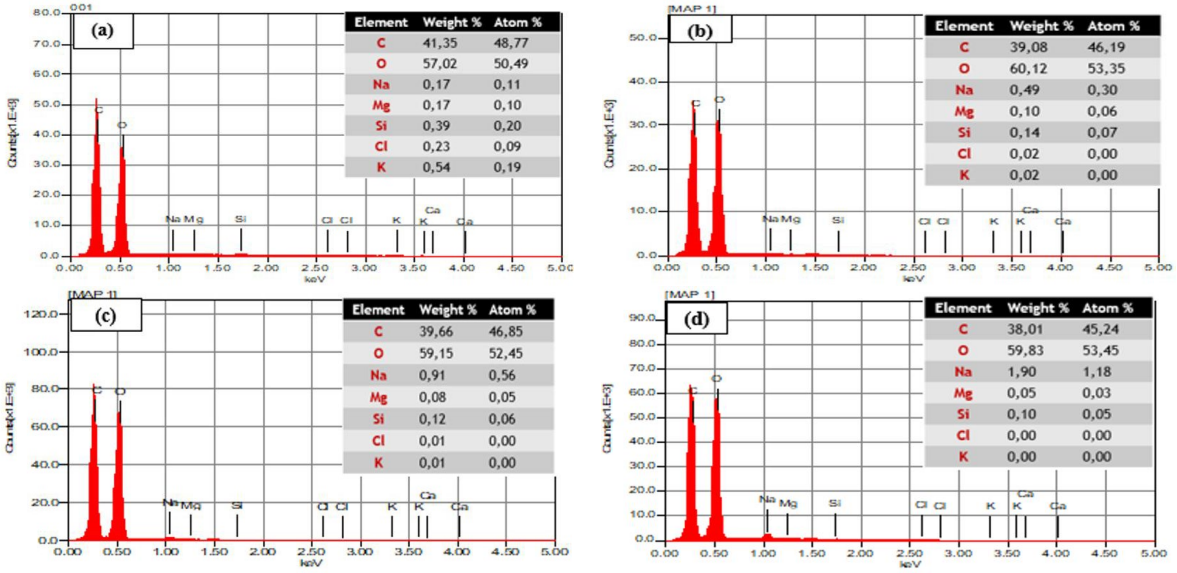

Figure 7: EDX analysis of (a) untreated, (b) 6%, (c) 12% and (d) 18% NaOH-treated SCB fibers

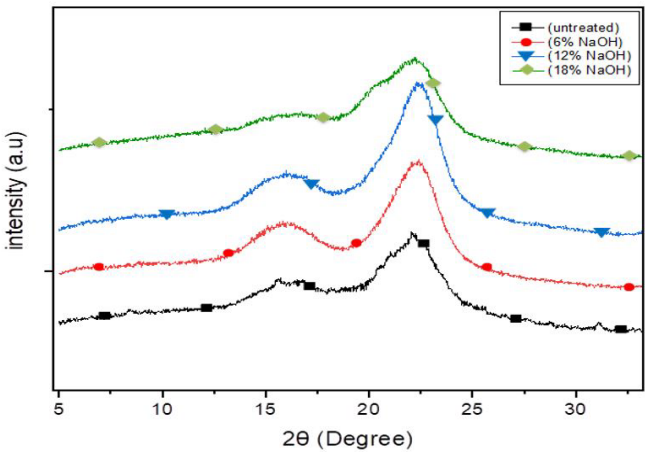

Figure 8: XRD patterns of untreated SCB fiber and fiber treated with 6%, 12%, and 18% NaOH

Table 5
XRD data for untreated and NaOH-treated sugarcane bagasse (SCB) fibers

NaOH concentration	2θ crystalline (°)	2θ amorphous (°)	%Cr	CrI	CS (nm)
0%	22.12	18.00	72.71	62.48	2.46
6%	22.17	18.64	78.20	72.13	2.78
12%	22.28	18.40	78.55	72.70	2.81
18%	22.24	18.10	72.44	61.96	2.59

X-ray diffraction (XRD) analysis

Table 5 and Figure 8 summarize the results of the diffraction patterns of untreated and NaOH-treated fibers, which reveal a peak at 2θ = 22°, corresponding to crystalline cellulose diffraction. Equations (1), (2), and (3) were used to obtain the percentage crystallinity (%Cr), crystallinity index (CrI), and crystallite size (CS). The untreated and treated SCB fibers with 6%, 12%, and 18% NaOH had CrI values of 62.48%, 72.13%, 72.70%, and 61.96%, respectively, while their %Cr values were 72.71%, 78.20%, 78.55%, and 72.44%, respectively. The treatment with 12% NaOH led to an 8.04% increase in %Cr and a 16.35% increase in CrI, compared to untreated fibers, but did not significantly affect CS. The improvement in %Cr, CrI, and CS observed in fibers treated with less than 12% NaOH can be attributed to the removal of excess amorphous regions, such as impurities, pectin, lignin, and hemicelluloses, which increased fiber crystallinity. However, excessive NaOH concentration (>12%) resulted in a decrease in %Cr, CrI, and CS, indicating cellulose deterioration and decreased crystallinity.[25]

Thermogravimetric analysis (TGA)

Figure 9 shows the results of TGA and DTG of both untreated and alkali-treated SCB fibers at different concentrations. The thermal degradation of fibers (treated and untreated) occurs in two stages, as illustrated by the two peaks in the DTG curve. The first stage occurs between 30 °C and 120 °C and is attributed to the loss of moisture. For untreated fibers, the first degradation peak is attributed to the degradation of hemicelluloses, as it was reported in the literature that it takes place between 200 °C and 350 °C; in our case, it took place between 150 °C and 240°C. The second degradation peak is assigned to the degradation of cellulose at 250 °C to 400 °C.[39] Fibers treated with 6%, 12%, and 18% NaOH showed only one peak between 308 °C and 317 °C, indicating that hemicelluloses were removed during the alkali treatment.[40]

The thermal degradation onsets of the raw and fibers treated with 6%, 12%, and 18 % NaOH are 191.82 °C, 277.58 °C, 269.92 °C, and 262.81 °C respectively (Table 6). The variation of the thermal degradation onset is related to the elimination of hemicelluloses, which is the least stable of the three major constituents of the fiber, it is also related to the destabilization of the native cellulose in 18% NaOH solution.

In addition, using TGA data, Broido's equation was used to determine the decomposition activation energy (Fig. 10). Table 7 shows that all treated fibers have higher activation energy values than untreated fibers. The activation energy of SCB treated with 6%

NaOH was 91.5 kJ/mol, which was the highest. Hence, SCB fiber treated with 6% NaOH is suitable for high-temperature applications due to its higher thermal stability.

Overall, the alkali treatment of SCB fibers enhanced the thermal stability, as the hemicelluloses (the unstable element) were eliminated. However, with severe alkali treatments (>6%), the native cellulose (cellulose I) was attacked, resulting in a lower temperature of cellulose degradation, and a consequent decrease in thermal stability.

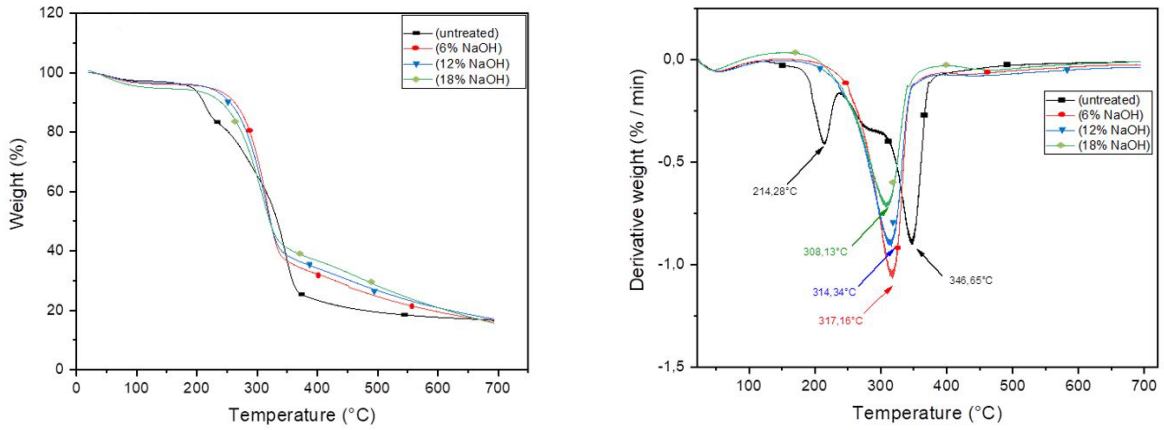

Figure 9: TG and DTG curves of untreated and alkali-treated SCB fibers

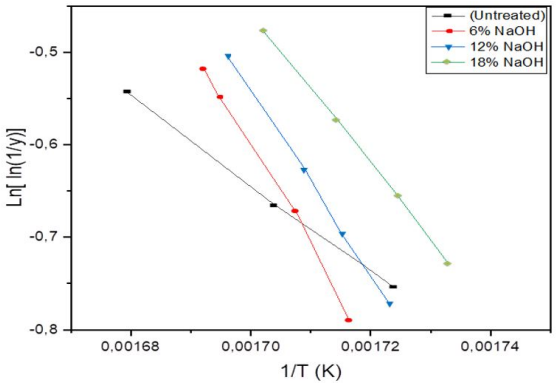

Figure 10: Broido's diagram for untreated and alkali-treated SCB fibers

Table 6
Thermal analysis data of raw and NaOH-treated SCB fibers

NaOH concentration	Onset temperature, °C	Endset temperature, °C	% Residues
0%	191.82	374.26	16.59
6%	277.18	358.57	16.27
12%	269.92	360.99	17.50
18%	262.81	366.98	15.65

Table 7
Kinetic activation energy of untreated and alkali-treated SCB fibers

NaOH concentration	Slope -(E/R)	Intercept	R^2	Equation	Activation energy (kJ/mol)
0%	-4703.3	7.3528	0.9993	y = -4703.3x + 7.3528	39.08
6%	-11006	18.108	0.9925	y = -11006x + 18.108	91.50
12%	-9967.6	16.403	0.9987	y = -9967.6x + 16.403	82.87
18%	-8127.2	13.358	0.9993	y = -8127.2x +13.358	67.56

Physical and mechanical properties

Table 8 presents the diameter and density data for both untreated and alkali-treated fibers, including other fiber types. The results demonstrate that as the concentration of alkali increases, the diameter of the fibers decreases. This reduction in diameter may be due to the breakdown of hemicelluloses and lignin, which weakens intermolecular interactions and separates fibers into fibrils.

Furthermore, the density of fibers treated with 6% alkali increased by 35.78% when compared to untreated fibers. This increase in density is likely due to the partial removal of non-cellulosic chemicals during the alkali treatment process.[9] Lignin and hemicelluloses are non-cellulosic components of natural fibers that provide structural support to the cell wall, but also create spaces between the cellulose fibers. When these components are removed with high concentrations of alkali, the cellulose fibers become more compacted, which changes the fiber's cell wall structure. The resulting fibers have a higher density because the cellulosic fibers aggregate more closely due to the high compaction, leading to an increase in weight per volume.[41]

The effect of the alkali treatment of sugarcane bagasse on tensile strength, strain at failure, and Young's modulus is summarized in Table 9 and plotted in Figure 11. The results indicate that Young's modulus of SCB fibers increases with alkali treatment up to 2% and decreases thereafter. In contrast, tensile strength and strain at failure increase with increasing NaOH concentration. The behaviors of strength and strain at failure are similar to those reported for raffia fiber,[48] fan palm fiber,[49] century fiber,[50] banana fiber,[51] red coconut empty fruit bunch fiber,[52] and *Borassus* fruit fine fiber.[53] Also, the behavior of Young's modulus of SCB fibers after the treatment is consistent with those observed in century fiber,[50] raffia fiber[48] and female date palm leaves.[54]

Sugarcane bagasse fibers, similarly to all other natural fibers, consist of several cells that are composed of cellulose crystalline microfibrils. Cellulose is interconnected with amorphous lignin and hemicelluloses.[55] Thus, severe alkali treatment (>2%) destroys the matrix of the fiber (lignin and hemicelluloses) and attacks cellulosic fibrils, causing a transition from native cellulose (cellulose I) to cellulose II.[56] Young's modulus of cellulose I is around 140 GPa, while that of cellulose II is only 90 GPa.[57]

Table 8
Comparison of diameter and density of alkali-treated and untreated sugarcane bagasse (SCB) with other natural fibers

Natural fibers	Diameter (μm)	Density (g/cm^3)
Untreated SCB	310±25	0.9253
6% treated SCB	214± 34	1.2564
12% treated SCB	185± 5	1.2977
18% treated SCB	160± 15	1.3101
Nigerian coir [42]	369 ± 5	1.097 ± 0.0125
Areca palm leaf stalk [43]	285–330	1.09 ± 0.024
Juncus effusus L. [44]	280 ± 56	1.139
Phoenix sp. [4]	576 ± 204	1.257 ± 0.062
Saharan aloe vera [45]	91.15	1.325
Furcraea foetida [46]	12.8	0.778
Corn husks [47]	186 ± 20	0.34

Table 9
Tensile properties of raw and alkali-treated sugarcane bagasse

NaOH concentration (%)	Tensile strength (MPa)	Strain at failure (%)	Young's Modulus (GPa)	Microfibrillar angle (°)
0	63 ± 22	3.03 ± 1.31	57 ± 22	14.03
2	118 ± 69	3.16 ± 1.08	101 ± 38	14.33
6	120 ± 67	3.27 ± 2.34	73 ± 24	14.57
12	142 ± 44	3.57 ± 1.56	60 ± 24	15.22
18	132 ± 89	4.66 ± 1.68	55 ± 16	17.35

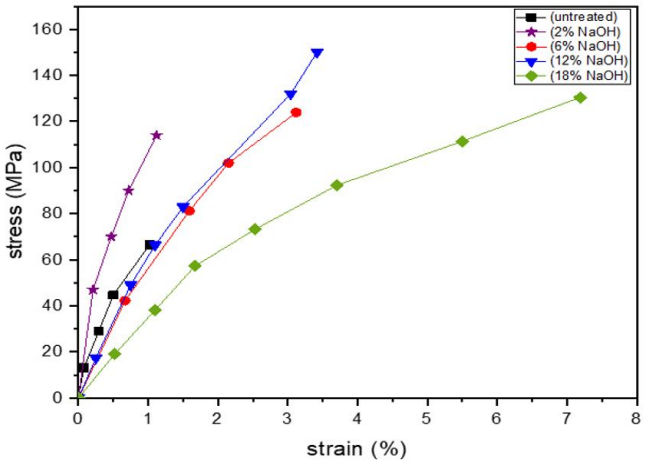

Figure 11: Stress-strain curves of untreated and alkali-treated SCB fibers

The treatment of fibers with 2% NaOH was conducted to demonstrate that treatment with low alkali concentration produces strong fibers compared to untreated fibers, considering that the treatment attacks only amorphous components leaving the crystalline cellulose intact. However, high alkali concentrations (>2%) result in weaker fibers due to the degradation of cellulose and the transition from cellulose I to cellulose II.

It was reported that the cell wall structure of the fiber differs in composition (ratio between cellulose and lignin/hemicelluloses), as well as in the orientation (microfibrillar angle) of the cellulose microfibrils.[55] Also, the effect of the microfibrillar angle was taken into consideration, which is calculated by Equation (6)[58] and reported in Table 8, where ε is the strain and α is the microfibrillar angle (°). The results show that the microfibrillar angle increases with the treatment, which explains the decrease in Young's modulus, showing that a strong negative correlation exists between the twist angle and Young's modulus.[59]

$$\varepsilon = -\ln(\cos\alpha) \quad (6)$$

Overall, the results of the previous structural and morphological analysis proved that the alkali treatment enhanced the thermal stability and ameliorated the morphology and structure of the fibers. However, the mechanical study showed that a severe treatment, even if it removes the amorphous components and impurities, may weaken the fibers. Consequently, an optimal NaOH solution should be chosen following mechanical tests.

Finite element analysis results

The results obtained from finite element analysis (FEA), as shown in Figure 12, represent the average values of 30 simulations for each RVE, considering the inherent uncertainties in the simulations. It should be noted that Young's modulus values correspond to PP/SCB composites with perfect interfacial bonding. Figure 11 illustrates that the PP reinforced with SCB fibers treated with a 2 wt% NaOH concentration exhibits the highest Young's modulus of 3755 ± 17 MPa, as hypothesized in the previous section. Moreover, SCB fibers treated with 6 wt% and 12 wt% NaOH concentrations also demonstrate elevated Young's modulus values compared to untreated fibers. However, severe treatment with an 18 wt% NaOH concentration weakens the SCB fibers, resulting in lower performance compared to the untreated fibers. Overall, the addition of SCB fibers enhances the Young's modulus of neat PP, which is 1300 MPa. This reinforcing effect is further augmented by the alkali treatment, which enhances the Young's modulus of the fibers and facilitates the transfer of stress between the fibers and the matrix.[60] However, it is important to employ a low alkali treatment concentration to avoid compromising the structural and mechanical properties of the fibers.

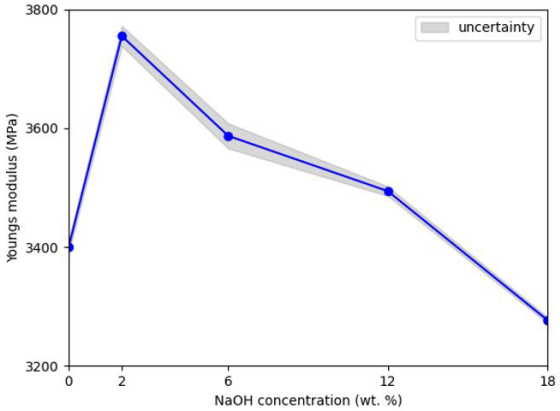

Figure 12: Effective Young's modulus of PP composites reinforced with untreated and alkali-treated SCB fibers

CONCLUSION

The study analyzed the chemical composition of SCB fibers before and after alkali treatment with three different concentrations (6%, 12%, and 18%). The results indicated a reduction in non-cellulosic substances and impurities. This was confirmed by FTIR and solid-state 13C NMR spectra. SEM analysis showed that treated fibers have cleaner and rougher surfaces. Additionally, XRD and TGA results indicated improved crystalline indexes and thermal stability in the treated fibers.

Based on these findings, it is recommended to use high NaOH concentrations (<18%) for treating natural fibers. However, mechanical testing revealed that excessive alkali treatment (>2%) led to weaker fibers, possibly due to the transformation of native cellulose into a different type (cellulose II), resulting in decreased Young's modulus. Therefore, the study suggests that low alkali treatment (<6%) produces strong fibers with good surface quality.

Finite element analysis predicted that incorporating 15 wt% of SCB fibers in the PP matrix enhanced the effective Young's modulus of PP/SCB composites. The optimal NaOH concentration showed the highest Young's modulus with 15 wt% of SCB in the PP matrix.

In conclusion, alkali-treated SCB fibers have the potential for various applications, which involve incorporating these agro-waste fillers into thermoplastic materials, due to their improved chemical, physical, and mechanical properties. Using SCB fibers as reinforcement presents an environmentally friendly alternative of synthetic fibers for use in industries like automobiles, aeronautics, and more.

REFERENCES

[1] S. Sathish, N. Karthi, L. Prabhu, S. Gokulkumar, D. Balaji *et al*., *Mater. Today Proc*., **45**, 8017 (2021), https://doi.org/10.1016/j.matpr.2020.12.1105

[2] V. Lakshmi Narayana and L. Bhaskara Rao, *Mater. Today Proc*., **44**, 1988 (2021), https://doi.org/10.1016/j.matpr.2020.12.117

[3] A. G. Adeniyi, D. V. Onifade, J. O. Ighalo and A. S. Adeoye, *Compos. Part B Eng*., **176**, 107305 (2019), https://doi.org/10.1016/j.compositesb.2019.107305

[4] G. Rajeshkumar, V. Hariharan and T. Scalici, *J. Nat. Fibers*, **13**, 702 (2016), https://doi.org/10.1080/15440478.2015.1130005

[5] N. F. Ismail, N. A. Mohd Radzuan, A. B. Sulong, N. Muhamad and C. H. Che Haron, *Polymers* (*Basel*), **13**, (2021), https://doi.org/10.3390/polym13122005

[6] H. Chen, Y. Yu, T. Zhong, Y. Wu, Y. Li *et al*., *Cellulose*, **24**, 333 (2017), https://doi.org/10.1007/s10570-016-1116-6

[7] X. Wang, L. Chang, X. Shi and L. Wang, *Materials* (*Basel*), **12**, (2019), https://doi.org/10.3390/ma12091386

[8] S. Mouhoubi, M. E. H. Bourahli, H. Osmani and S. Abdeslam, *J. Nat. Fibers*, **14**, 239 (2017), https://doi.org/10.1080/15440478.2016.1193088

[9] C. Tenazoa, H. Savastano, S. Charca, M. Quintana and E. Flores, *J. Nat. Fibers*, **18**, 923 (2021), https://doi.org/10.1080/15440478.2019.1675211

[10] H. Chen, J. Wu, J. Shi, W. Zhang and H. Wang, *Ind. Crop. Prod*., **164**, (2021), https://doi.org/10.1016/j.indcrop.2021.113380

[11] A. Oushabi, S. Sair, F. Oudrhiri Hassani, Y. Abboud, O. Tanan *et al*., *South Afr. J. Chem. Eng*., **23**, 116 (2017), https://doi.org/10.1016/j.sajce.2017.04.005

[12] L. Segal, J. J. Creely, A. E. Martin and C. M. Conrad, *Text. Res. J*., **29**, 786 (1959), https://doi.org/10.1177/004051755902901003

[13] E. Xu, D. Wang and L. Lin, *Forests*, **11**, (2020), https://doi.org/10.3390/f11010087

[14] A. Broido, *J. Polym. Sci. Part A-2 Polym. Phys*., **7**, 1761 (1969), https://doi.org/10.1002/pol.1969.160071012

[15] Z. Sadik, E. Ablouh, M. Sadik, K. Benmoussa, H. Idrissi-Saba *et al*., *Eng*. *Solid Mech*. **8**, 233 (2020), https://doi.org/10.5267/j.esm.2020.1.001
[16] A. El Moumen, F. N'Guyen, T. Kanit and A. Imad, *Mech*. *Mater*., **145**, 103348 (2020), https://doi.org/10.1016/j.mechmat.2020.103348
[17] F. Z. Arrakhiz, M. El Achaby, K. Benmoussa, R. Bouhfid, E. M. Essassi *et al*., *Mater*. *Des*., **40**, 528 (2012), https://doi.org/10.1016/j.matdes.2012.04.032
[18] S. S. Munawar, K. Umemura and S. Kawai, *J. Wood Sci*., **53**, 108 (2007), https://doi.org/10.1007/s10086-006-0836-x
[19] N. Venkateshwaran and A. Elayaperumal, *J. Reinf. Plast. Compos*., **29**, 2387 (2010), https://doi.org/10.1177/0731684409360578
[20] I. M. De Rosa, C. Santulli and F. Sarasini, *Mater. Des*., **31**, 2397 (2010), https://doi.org/10.1016/j.matdes.2009.11.059
[21] M. J. John and R. D. Anandjiwala, *Polym. Polym. Compos*., **16**, 101 (2008), https://doi.org/10.1002/pc
[22] X. Li, L. G. Tabil and S. Panigrahi, *J. Polym. Environ*., **15**, 25 (2007), https://doi.org/10.1007/s10924-006-0042-3
[23] F. de A. Silva, N. Chawla and R. D. de T. Filho, *Compos. Sci. Technol*., **68**, 3438 (2008), https://doi.org/10.1016/j.compscitech.2008.10.001
[24] K. Obi Reddy, G. Sivamohan Reddy, C. Uma Maheswari, A. Varada Rajulu and K. Madhusudhana Rao, *J. For. Res*., **21**, 53 (2010), https://doi.org/10.1007/s11676-010-0008-0
[25] K. Raja, B. Prabu, P. Ganeshan, V. S. Chandra Sekar and B. Nagaraja Ganesh, *J. Nat. Fibers*, **18**, 1934 (2021), https://doi.org/10.1080/15440478.2019.1710650
[26] R. Vijay, S. Manoharan, S. Arjun, A. Vinod and D. L. Singaravelu, *J. Nat. Fibers*, **18**, 1957 (2021), https://doi.org/10.1080/15440478.2019.1710651
[27] B. Nagaraja Ganesh, P. Ganeshan, P. Ramshankar and K. Raja, *Ind. Crop. Prod*., **139**, 111546 (2019), https://doi.org/10.1016/j.indcrop.2019.111546
[28] C. E. Njoku, J. A. Omotoyinbo, K. K. Alaneme and M. O. Daramola, *J. Nat. Fibers*, **19**, 485 (2022), https://doi.org/10.1080/15440478.2020.1745127
[29] T. M. Loganathan, M. T. H. Sultan, Q. Ahsan, M. Jawaid, J. Naveen *et al*., *J. Mater. Res. Technol*., **9**, 3537 (2020), https://doi.org/10.1016/j.jmrt.2020.01.091
[30] Y.-H. Feng, T.-Y. Cheng, W.-G. Yang, P.-T. Ma, H.-Z. He *et al*., *Ind. Crop. Prod*., **111**, 285 (2018), https://doi.org/10.1016/j.indcrop.2017.10.041
[31] M. Lara-Serrano, S. Morales-delaRosa, J. M. Campos-Martín and J. L. G. Fierro, *Appl. Sci*., **9**, (2019), https://doi.org/10.3390/app9091862
[32] B. Nagarajaganesh and B. Rekha, *Mater. Res. Express*, **6**, (2019), https://doi.org/10.1088/2053-1591/ab5395
[33] M. Stanzione, M. Oliviero, M. Cocca, M. E. Errico, G. Gentile *et al*., *Carbohyd. Polym*., **231**, 115772 (2020), https://doi.org/10.1016/j.carbpol.2019.115772
[34] J. Fu, C. He, C. Jiang and Y. Chen, *BioResources*, **14**, 6384 (2019), https://doi.org/10.15376/biores.14.3.6384-6396
[35] K. O. Reddy, C. U. Maheswari, M. Shukla and A. V. Rajulu, *Mater. Lett*., **67**, 35 (2012), https://doi.org/10.1016/j.matlet.2011.09.027
[36] B. A. Obi Reddy, *Mech. Eng. Technol*., **4**, 1 (2011), https://doi.org/10.1016/j.carbpol.2018.01.110
[37] K. E. Borchani, C. Carrot and M. Jaziri, *Cellulose*, **22**, 1577 (2015), https://doi.org/10.1007/s10570-015-0583-5
[38] P. Manimaran, M. R. Sanjay, P. Senthamaraikannan, M. Jawaid, S. S. Saravanakumar *et al*., *J. Nat. Fibers*, **16**, 768 (2019), https://doi.org/10.1080/15440478.2018.1434851
[39] J. L. Thomason and J. L.Rudeiros-Fernández, *Polym. Degrad. Stabil*., **188** (2021), https://doi.org/10.1016/j.polymdegradstab.2021.109594
[40] L. Xia, C. Zhang, A. Wang, Y. Wang and W. Xu, *Cellulose*, **27**, 1909 (2020), https://doi.org/10.1007/s10570-019-02933-9
[41] F. Serra-Parareda, Q. Tarrés, F. X. Espinach, F. Vilaseca, P. Mutjé *et al*., *Int. J. Biol. Macromol*., **155**, 81 (2020), https://doi.org/10.1016/j.ijbiomac.2020.03.160
[42] C. O. Akintayo, M. A. Azeez, S. Beuerman and E. T. Akintayo, *J. Nat. Fibers*, **13**, 520 (2016), https://doi.org/10.1080/15440478.2015.1076365
[43] N. Shanmugasundaram, I. Rajendran and T. Ramkumar, *Carbohyd. Polym*., **195**, 566 (2018), https://doi.org/10.1016/j.carbpol.2018.04.127
[44] M. Maache, A. Bezazi, S. Amroune, F. Scarpa and A. Dufresne, *Carbohyd. Polym*., **171**, 163 (2017), https://doi.org/10.1016/j.carbpol.2017.04.096
[45] A. N. Balaji and K. J. Nagarajan, *Carbohyd. Polym*., **174**, 200 (2017), https://doi.org/10.1016/j.carbpol.2017.06.065
[46] P. Manimaran, P. Senthamaraikannan, M. R. Sanjay, M. K. Marichelvam and M. Jawaid, *Carbohyd. Polym*., **181**, 650 (2018), https://doi.org/10.1016/j.carbpol.2017.11.099
[47] N. Herlina Sari, I. N. G. Wardana, Y. S. Irawan and E. Siswanto, *J. Nat. Fibers*, **15**, 545 (2018), https://doi.org/10.1080/15440478.2017.1349707
[48] R. G. Elenga, P. Djemia, D. Tingaud, T. Chauveau, J. G. Maniongui *et al*., *BioResources*, **8**, 2934 (2013), https://doi.org/10.15376/biores.8.2.2934-2949
[49] M. Machaka, H. Abou Chakra and A. Elkordi, *Eur. Sci. J*., **10**, 1857 (2014)
[50] K. O. Reddy, K. R. N. Reddy, J. Zhang and A. Varada Rajulu, *J. Nat. Fibers*, **10**, 282 (2013), https://doi.org/10.1080/15440478.2013.800812
[51] M. Khan, S. Rahamathbaba, M. A. Mateen, D. V. Ravi Shankar and M. Manzoor Hussain, *Polym. Renew. Resour*., **10**, 19 (2019), https://doi.org/10.1177/2041247919863626
[52] K. J. Nagarajan and A. N. Balaji, *Int. J. Polym. Anal. Charact*., **21**, 387 (2016),

https://doi.org/10.1080/1023666X.2016.1160814
[53] K. Obi Reddy, C. Uma Maheswari, M. Shukla, J. I. Song and A. Varada Rajulu, *Compos*. *Part B Eng*., **44**, 433 (2013), https://doi.org/10.1016/j.compositesb.2012.04.075
[54] M. A. Al Maadeed, R. Kahraman, P. Noorunnisa Khanam and S. Al-Maadeed, *Mater*. *Des*., **43**, 526 (2013), https://doi.org/10.1016/j.matdes.2012.07.028
[55] A. K. Bledzki and J. Gassan, *Prog*. *Polym*. *Sci*., **24**, 221 (1999), https://doi.org/10.1016/S0079-6700(98)00018-5
[56] A. El Oudiani, Y. Chaabouni, S. Msahli and F. Sakli, *Carbohyd*. *Polym*., **86**, 1221 (2011), https://doi.org/10.1016/j.carbpol.2011.06.037
[57] M. G. Northolt, H. Boerstoel, H. Maatman, R. Huisman, J. Veurink *et al*., *Polymer* (*Guildf*), **42**, 8249 (2001), https://doi.org/10.1016/S0032-3861(01)00211-7
[58] K. Charlet, S. Eve, J. P. Jernot, M. Gomina and J. Breard, *Proc*. *Eng*., **1**, 233 (2009), https://doi.org/10.1016/j.proeng.2009.06.055
[59] A. Bourmaud, C. Morvan, A. Bouali, V. Placet, P. Perré *et al*., *Ind*. *Crop*. *Prod*., **44**, 343 (2013), https://doi.org/10.1016/J.INDCROP.2012.11.031
[60] V. Fiore, G. Di Bella and A. Valenza, *Compos*. *Part B Eng*., **68**, 14 (2015), https://doi.org/10.1016/j.compositesb.2014.08.025